Open access • Journal Article • DOI:10.1061/(ASCE)GM.1943-5622.0000284

Elastic-viscoplastic modeling for natural soft clays considering nonlinear creep

Zhen-Yu Yin, Qiang Xu, Chuang Yu

Institutions: Chengdu University of Technology, Wenzhou University

Published on: 01 Oct 2015 - International Journal of Geomechanics (American Society of Civil Engineers)

Topics: Creep, Oedometer test and Viscoplasticity

Elastic-viscoplastic modeling for natural soft clays considering nonlinear creep

Zhenyu Yin, Qiang Xu, Chuang Yu

Elastic-Viscoplastic Modeling for Natural Soft Clays Considering Nonlinear Creep

Zhen-Yu Yin[1]; Qiang Xu[2]; and Chuang Yu[3]

Abstract: This paper focuses on nonlinear creep behavior with a consecutively decreasing creep coefficient $C_{\alpha e}$ fully related to the soil density. Conventional oedometer tests on reconstituted samples of several natural soft clays are selected to clarify the evolution of creep coefficient throughout testing. On this basis, a simple nonlinear creep formulation is proposed accounting for the effect of volumetric packing of soil assemblies. The formulation is then incorporated into a newly developed elastic-viscoplastic model to take into account the nonlinear creep of natural soft clays. One additional parameter is added that can be determined in a straightforward way from an oedometer test without additional experimental cost. The enhanced nonlinear creep model is examined by simulating a conventional oedometer test on reconstituted Haarajoki clay. The improvement of predictions by the nonlinear creep formulation is highlighted by comparing predictions with constant $C_{\alpha e}$. The enhanced model is further applied to Murro test embankment. The influence of consideration of nonlinear creep on the embankment behavior is discussed.

Author keywords: Clays; Constitutive models; Creep; Embankments; Laboratory tests; Numerical analysis; Viscoplasticity.

Introduction

Natural soft clays exhibit significant time-dependent deformations under both laboratory and in situ conditions after primary consolidation owing to viscosity (e.g., Bjerrum 1967; Mesri and Godlewski 1977; Graham et al. 1983; Leroueil et al. 1985; Yin 1999; Augustesen et al. 2004; Yin and Hicher 2008; Li et al. 2009; Karstunen and Yin 2010; Desai et al. 2011). The creep coefficient $C_{\alpha e}$ (defined as $C_{\alpha e} = \Delta e / \Delta \ln t$ based on one-dimensional creep test) is commonly used explicitly or implicitly in the development of viscoplastic models and in practice (e.g., Adachi and Oka 1982; Yin and Graham 1989; Kutter and Sathialingam 1992; Vermeer and Neher 1999; Leoni et al. 2008; Yin et al. 2010, 2011b, c). A constant $C_{\alpha e}$ was generally considered in such formulations. To overcome the limitation of infinite strains up to a negative void ratio during creep, Yin et al. (2002) successfully formulated a nonlinear $C_{\alpha e}$ with time for one applied stress level, which was subsequently adopted by Kelln et al. (2008). However, the nonlinear $C_{\alpha e}$ does not consecutively decrease with void ratio when applied stresses are increased. As a result, the models can avoid a negative void ratio during creep under a constant stress level but not for the condition of varying stresses, which is common during constructions.

Therefore, this paper focuses on nonlinear creep behavior with a consecutively decreasing $C_{\alpha e}$ fully related to the soil density. Conventional oedometer tests on different soft clays are investigated to propose a simple nonlinear creep formulation. All selected tests are on reconstituted samples to eliminate the influence of soil structure on the evolution of $C_{\alpha e}$. Using the proposed formulation, an enhanced elastic-viscoplastic (EVP) model is then developed accounting for the nonlinear creep behavior. The influence of the nonlinear creep consideration on modeling a laboratory test and an in situ test is discussed.

Nonlinear Creep Formulation

Evidence of Nonlinear Creep Behavior

Conventional oedometer tests on five Finnish clays were selected for this study (see Karstunen and Koskinen 2008; Stapelfeldt et al. 2007, 2008; Karstunen and Yin 2010; Yin et al. 2011b). All selected tests are on reconstituted samples to eliminate the influence of soil structure. Some physical properties of selected clays are summarized in Table 1. The results of all selected conventional oedometer tests are presented in Fig. 1, including e-log σ'_v curves, $C_{\alpha e}$-log σ'_v curves, and $C_{\alpha e}$-$(\lambda - \kappa)$ curves (e, void ratio; λ, compression index; κ, swelling index):

1. From e-log σ'_v curves, although there is variation of initial void ratio for all selected clays, for each clay the compressibility of different samples is almost identical with regard to compression lines in each figure from *a* to *e*.
2. The averaged $C_{\alpha e}$ was measured within the time interval from 4–24 h for each applied stress level and plotted against the σ'_v in logarithmic scale for normally consolidated states (applied stresses are bigger than the preconsolidation pressure: $\sigma'_v > \sigma'_{p0}$). All results show that the measured $C_{\alpha e}$ is consecutively decreasing with the increasing applied stress level, which may be attributable to the increasing density when soils are compressed.
3. Mesri and Godlewski (1977) suggested plotting the $C_{\alpha e}$-λ curve to study the time and stress-compressibility interrelationship. Because the $C_{\alpha e}$ includes only the inelastic deformation, this study suggests plotting the $C_{\alpha e}$-$(\lambda - \kappa)$ curve,

[1]Associate Professor, Lunan Univ., Ecole Centrale de Nantes, UMR CNRS GeM, Nantes, France; Invited Professor, State Key Laboratory of Geohazard Prevention and Geoenvironment Protection, Chengdu Univ. of Technology, Chengdu 610059, China; formerly, Professor, Dept. of Civil Engineering, Shanghai Jiao Tong Univ., Shanghai 200240, China (corresponding author). E-mail: zhenyu.yin@gmail.com

[2]Professor, State Key Laboratory of Geohazard Prevention and Geoenvironment Protection, Chengdu Univ. of Technology, Chengdu 610059, China.

[3]Associate Professor, Dept. of Civil Engineering, Wenzhou Univ., Wenzhou 325035, China.

Table 1. Average Values of Physical and Mechanical Characteristics of Selected Clays

Clays	γ (kN/m^3)	w (%)	w_P (%)	w_L (%)	e_0	κ	λ	$C_{\alpha e0}$	m
Murro clay	15.3	77	34	88	2.02	0.028	0.216	0.0147	0.73
Vanttila clay	13.6	115	30	98	2.42	0.06	0.288	0.0185	0.82
Haarajoki clay	14.2	87	26	88	2.63	0.046	0.369	0.027	2.12
Suurpelto clay	14.3	72	23	80	2.52	0.04	0.335	0.0293	2.19
Mixed clay[a]	17.7	43	26	45	1.16	0.022	0.113	0.0035	1.36
HKMC	—	57	28	60	1.5	0.03	0.201	0.0084	1.09

[a]Mixed clay is a mixture of different clays from Southern Finland, reported in text by Stapelfeldt et al. (2007).

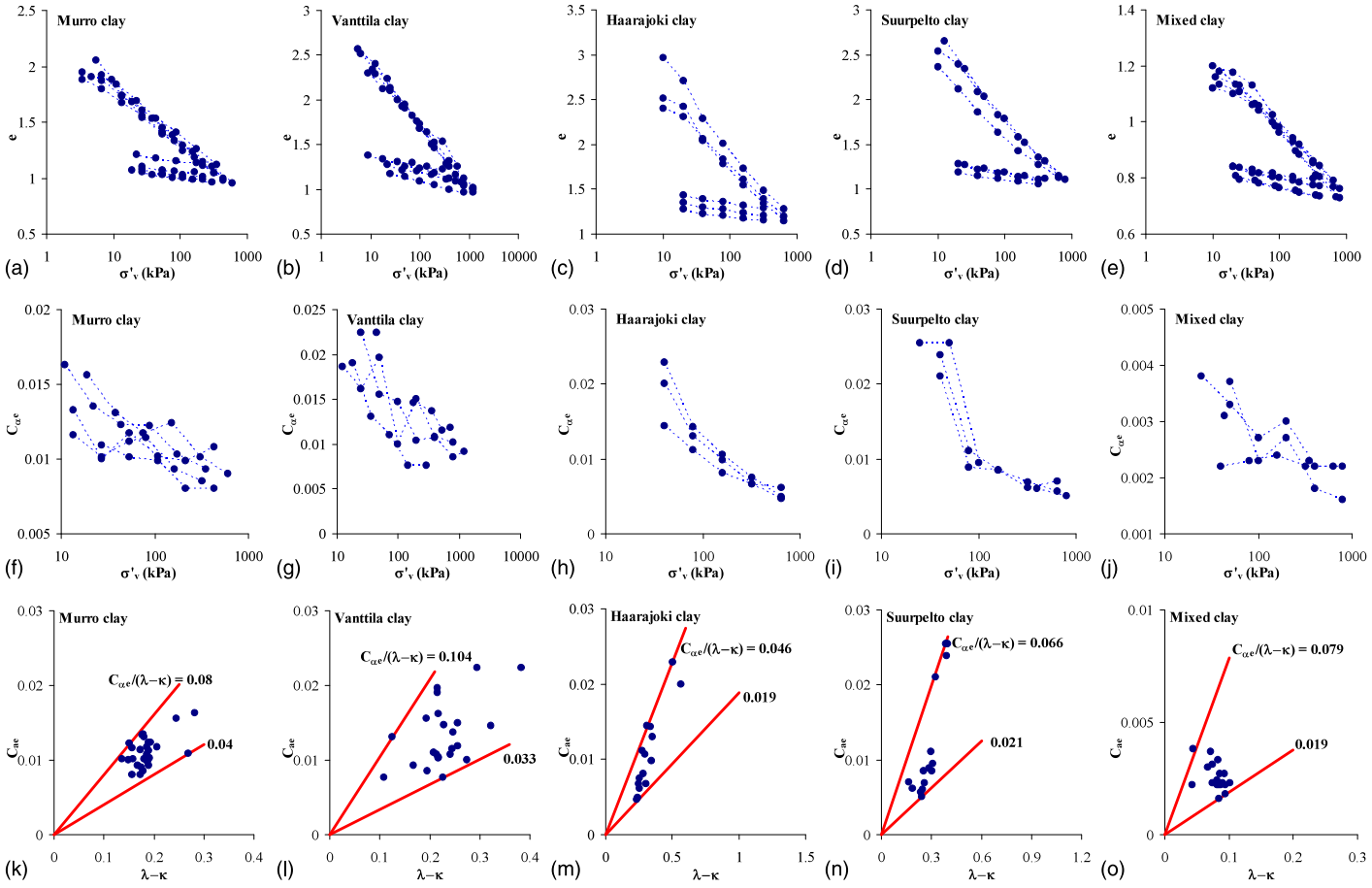

Fig. 1. Results of conventional oedometer tests on different reconstituted clays: (a)–(e) void ratio versus vertical effective stress in logarithmic scale; (f)–(j) creep coefficient versus vertical effective stress in logarithmic scale; (k)–(o) creep coefficient versus compressibility index

where $(\lambda - \kappa)$ includes only inelastic deformation similar to $C_{\alpha e}$ (κ is determined from unloading curve). All results show varying ratios of $C_{\alpha e}/(\lambda - \kappa)$ for all clays. Because the $(\lambda - \kappa)$ is almost constant for each clay, the variation of $C_{\alpha e}/(\lambda - \kappa)$ is caused by the evolution of $C_{\alpha e}$ with applied stress level or soil density.

Limitation of Current Approaches

To describe the variation of the creep coefficient $C_{\alpha e}$ during creep under one applied stress level, Yin (1999) proposed a nonlinear creep formulation [Eq. (1)] based on test results on Hong Kong marine clay (HKMC):

$$C_{\alpha e} = \frac{C_{\alpha e0}}{1 + \dfrac{C_{\alpha e0}}{V \Delta \varepsilon_{vl}} \ln\left(\dfrac{t_c + t_{\mathrm{EOP}}}{t_{\mathrm{EOP}}}\right)} \tag{1}$$

where $V = 1 + e_0$ (with e_0 representing the initial void ratio); $C_{\alpha e0}$ = initial value of $C_{\alpha e}$; $\Delta\varepsilon_{vl}$ = creep strain limit controlling the diminution rate of $C_{\alpha e}$; t_{EOP} = time up to the end of primary consolidation; and t_c = creep time of test taken equal to $t - t_{\mathrm{EOP}}$. The Eq. (1) indicates a decreasing $C_{\alpha e}$ with time under a constant stress state.

This formulation was further developed for a three-dimensional creep model by Yin et al. (2002), with the creep volumetric strain rate $\dot{\varepsilon}_v^{vp}$ expressed as follows:

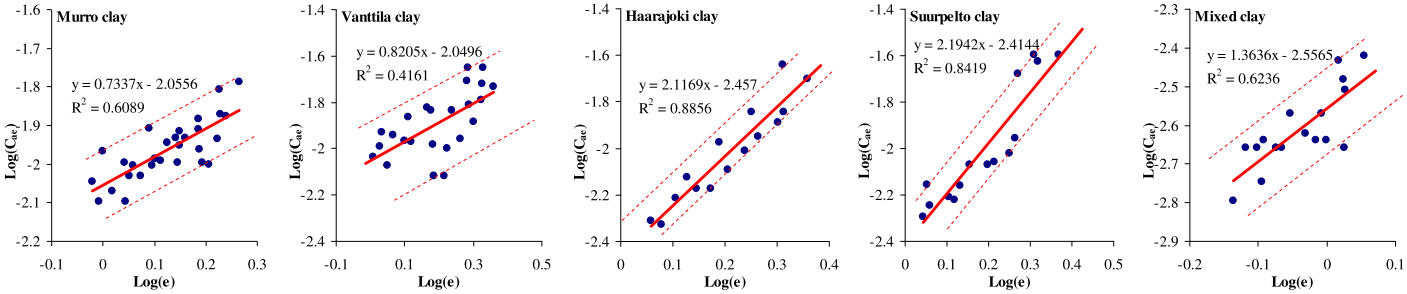

Fig. 2. Creep coefficient versus void ratio in double logarithmic scale for different clays

$$\dot{\varepsilon}_v^{vp} = \frac{C_{\alpha e0}}{V\tau}\left(1+\frac{\varepsilon_{vm}^r-\varepsilon_{vm}}{\varepsilon_{vml}^{vp}}\right)^2 \exp\left[\frac{\varepsilon_{vm}^r-\varepsilon_{vm}}{\left(1+\frac{\varepsilon_{vm}^r-\varepsilon_{vm}}{\varepsilon_{vml}^{vp}}\right)}\frac{V}{C_{\alpha e0}}\right] \quad (2)$$

where τ = reference time ($\tau = 1$ day for a conventional oedometer test); ε_{vm} = volumetric strain corresponding to the current mean effective stress p_m; ε_{vm}^r = reference volumetric strain corresponding to p_m by $\varepsilon_{vm}^r = \varepsilon_{vm0}^r + (\lambda/V)\ln(p_m/p_{m0})$, with initial reference mean effective stress p_{m0}, initial reference volumetric strain ε_{vm0}^r, and compression index λ; and ε_{vml}^{vp} = limit creep strain equal to $e_0/(1+e_0)$. More recently, Kelln et al. (2008) have extended the formulation using specific volumes instead of strains. The advantage of the proposed formulation is to describe a decreasing creep coefficient $C_{\alpha e}$ by time for one applied stress level without an additional material constant. For a conventional oedometer test, the $C_{\alpha e} = C_{\alpha e0}$ is implied in Eq. (2) at $t = \tau$ when the current stress-void ratio state equals the corresponding reference state ($\varepsilon_{vm} = \varepsilon_{vm}^r$).

However, when the stress state is changed, a new reference volumetric strain ε_{vm}^r is calculated owing to the new p_m, and, in turn, the $C_{\alpha e}$ starts with a bigger value and decreases to the value $C_{\alpha e0}$ at $t = \tau$, even for more-compressed soils with increased ε_{vm}. In other words, the creep formulation, Eq. (2), describes only the nonlinear evolution of $C_{\alpha e}$ by time for a constant applied stress level, but is changed back when the applied stresses are changed. For instance, in the case of predicting a conventional oedometer test, the $C_{\alpha e}$ is always taken equal to the value $C_{\alpha e0}$ at $t = \tau$ for all applied stress levels bigger than the preconsolidation pressure. Thus, the consecutively decreasing $C_{\alpha e}$ with applied stress or soil density cannot be reproduced.

Proposed Nonlinear Creep Formulation

Because the void ratio is a physical state of soils representing soil density and deformation potential, the averaged $C_{\alpha e}$ was further plotted against the void ratio in double logarithmic space, as shown in Fig. 2. On this basis, a new nonlinear creep formulation can be proposed as follows:

$$\frac{C_{\alpha e}}{C_{\alpha ef}} = \left(\frac{e}{e_f}\right)^m \quad (3)$$

where $C_{\alpha ef}$ and e_f = reference values of creep coefficient and void ratio, respectively; and m = material constant representing the slope of the $\log(C_{\alpha e})$-$\log(e)$ curve, which can be measured in a straightforward way. For simplicity, the initial void ratio e_0 can be used for e_f, and then the initial value $C_{\alpha e0}$ obtained from Fig. 2 can be used for $C_{\alpha ef}$. Values of $C_{\alpha e0}$ and m for all selected clays are summarized in Table 1. Furthermore, the correlations between m and Atterberg limits were investigated based on available results. Fig. 3 shows the material constant m can be approximately determined by the plastic limit of soils by a simple power-type formula. Note that, lacking a large quantity of data, the correlation needs to be further investigated with liquid limit or plasticity index at both macrophenomena and microstructure levels (see Yin and Chang 2009; Yin et al. 2009, 2011a).

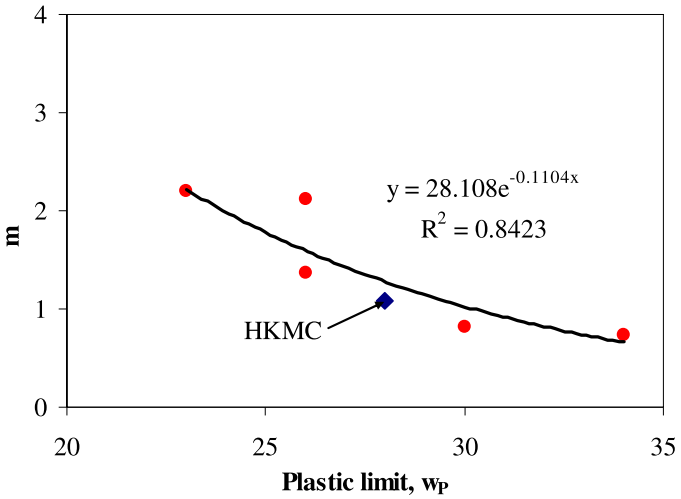

Fig. 3. Evolution of material constant m with plastic limit

The Eq. (3) implies (1) a decreasing $C_{\alpha e}$ by time for an applied stress level when the void ratio is decreasing during creep, and (2) a consecutively decreasing $C_{\alpha e}$ with applied stresses when the void ratio is consecutively decreasing during loading. Furthermore, as the void ratio approaches zero, the creep rate $C_{\alpha e}$ also approaches zero, which can in turn keep the void ratio positive.

As indicated in Fig. 1, the variation of $C_{\alpha e}/(\lambda-\kappa)$ is attributable to the nonlinear creep coefficient related to the void ratio. Thus, this variation can be plotted in the space of $(\lambda-k)/C_{\alpha e}$-e, where the term $(\lambda-\kappa)/C_{\alpha e}$ is more commonly used as a rate-dependency parameter of viscoplastic models (see, among others, Kutter and Sathialingam 1992; Vermeer and Neher 1999; Leoni et al. 2008; Yin et al. 2010, 2011b). Applying the proposed nonlinear creep formulation Eq. (3) to $C_{\alpha e}$, the theoretical curves were plotted (solid lines in Fig. 4), which fit well with experimental data.

Application to HKMC

The conventional oedometer test on HKMC by Yin (1999) was selected for the application of the previously described analyses. The test results are presented in Fig. 5.

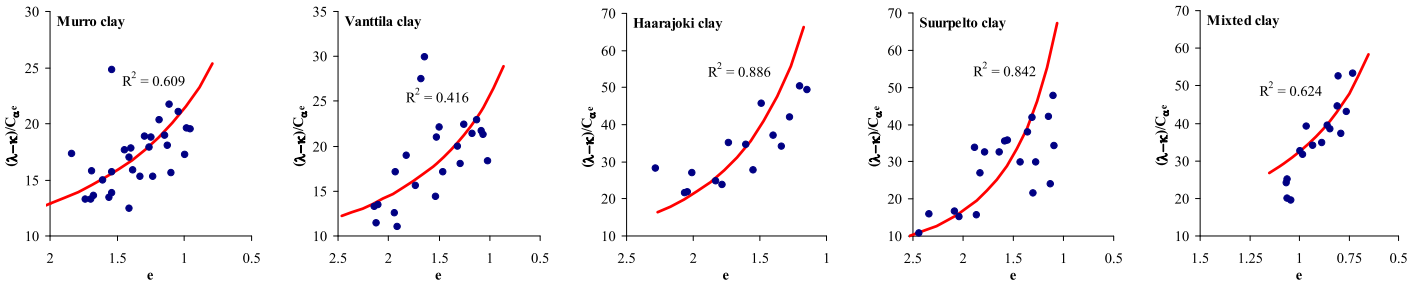

Fig. 4. Evolution of ratio $C_{\alpha e}/(\lambda-\kappa)$ with void ratio for different clays

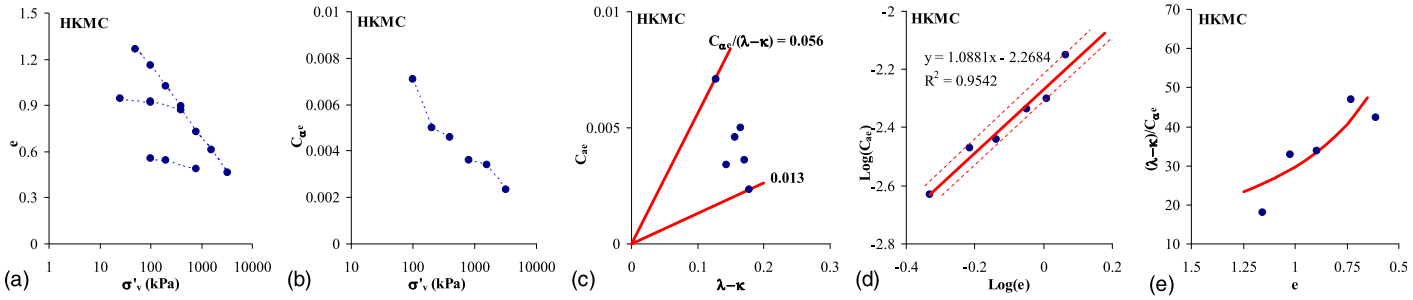

Fig. 5. Results of conventional oedometer test on HKMC: (a) void ratio versus vertical effective stress in logarithmic scale; (b) creep coefficient versus vertical effective stress in logarithmic scale; (c) creep coefficient versus compressibility index; (d) creep coefficient versus void ratio in double logarithmic scale; (e) ratio of $C_{\alpha e}/(\lambda-\kappa)$ versus void ratio

The compressibility index κ and λ were obtained from the e-log σ'_v curve [Fig. 5(a)]. The averaged $C_{\alpha e}$, which is consecutively decreasing with the increasing applied stresses, was measured [Fig. 5(b)]. The averaged $C_{\alpha e}$ was then plotted with $(\lambda-\kappa)$, which shows a variation of the ratio $C_{\alpha e}/(\lambda-\kappa)$ owing to the evolution of $C_{\alpha e}$ with soil density [Fig. 5(c)]. The averaged $C_{\alpha e}$ was further plotted against the void ratio in double logarithmic space, from which the $C_{\alpha e0}$ and m were obtained [Fig. 5(d) and Table 1]. The value $m = 1.09$ obtained from the test is found to be close to that obtained by the correlation ($m = 1.27$; Fig. 3). Using Eq. (3), the theoretical curve for $(\lambda-\kappa)/C_{\alpha e}$ plotted with e fits well with experimental data [Fig. 5(e)]. All results demonstrate that the proposed nonlinear formulation with the correlation for m is suitable for HKMC.

EVP Model Considering Nonlinear Creep

In this section, the proposed nonlinear creep formulation is incorporated into a newly developed EVP model (Yin et al. 2010, 2011b) to take into account the nonlinear creep behavior of natural soft clays.

Brief Introduction of EVP Model

Because natural soft clays exhibit significant features of anisotropy, destructuration, and viscosity, a new EVP model based on the strain-rate dependency of preconsolidation pressure has been developed and validated by Yin et al. (2010, 2011b). The model has advantages on describing the full coupling of all three previously mentioned features and the straightforward determination of parameters with the same cost as the modified Cam-clay model (Roscoe and Burland 1968). As indicated by Kutter and Sathialingam (1992), this kind of model follows the hypothesis of Bjerrum (1967) that there is no instant in elastic strains, which does not mean the delayed compression does not occur before the completion of primary consolidation.

The model principle is illustrated in Fig. 6. The brief introduction of the model with constitutive equations and parameters can be found in the Appendix. More details can be found in Yin et al. (2010, 2011b). It is worth pointing out that the key constitutive equation accounting for creep behavior is Eq. (9) combined with Eq. (15), which can be expressed as follows:

$$\dot{\varepsilon}_{ij}^{vp} = \frac{C_{\alpha ei}}{(1+e_0)\tau}\frac{\left(M_c^2-\alpha_{K0}^2\right)}{\left(M_c^2-\eta_{K0}^2\right)}\left(\frac{p_m^d}{p_m^r}\right)^{(\lambda_i-\kappa)/(C_{\alpha ei})}\frac{\partial f_d}{\partial \sigma'_{ij}} \tag{4}$$

with $C_{\alpha e}$ replaced by $C_{\alpha ei}$ defined from the conventional oedometer test on reconstituted clays.

Incorporation of Nonlinear Creep Formulation

As discussed in previous sections, for reconstituted clays the creep coefficient $C_{\alpha e}$ is decreasing with the diminution of void ratio, which can cause an increasing ratio of $(\lambda-\kappa)/C_{\alpha e}$. Unifying the symbols $C_{\alpha e}$ of reconstituted clays by $C_{\alpha ei}$ and using the initial void ratio e_0, Eq. (3) is rewritten as follows:

$$C_{\alpha ei} = C_{\alpha ei0}\left(\frac{e}{e_0}\right)^m \tag{5}$$

Substituting Eq. (5) into Eq. (4), the viscoplastic strain rate can be expressed as follows:

$$\dot{\varepsilon}_{ij}^{vp} = \frac{C_{\alpha ei0}}{(1+e_0)\tau}\left(\frac{e}{e_0}\right)^m\frac{\left(M_c^2-\alpha_{K_0}^2\right)}{\left(M_c^2-\eta_{K_0}^2\right)}\left(\frac{p_m^d}{p_m^r}\right)^{[(\lambda_i-\kappa)/(C_{\alpha ei0})](e_0/e)^m}\frac{\partial f_d}{\partial \sigma'_{ij}} \tag{6}$$

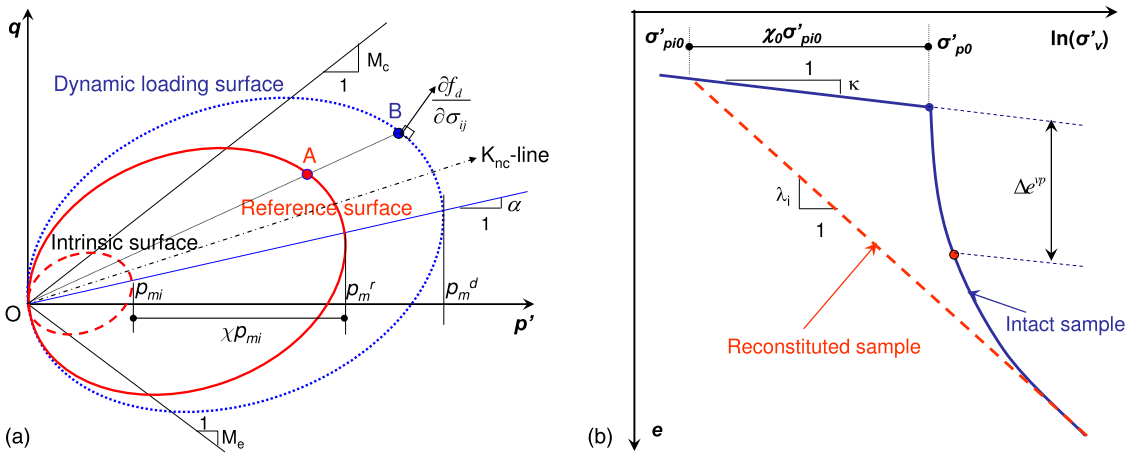

Fig. 6. Illustrations of model principle: (a) defined in p'-q space; (b) defined in e-ln(σ'_v) space

Combined with other constitutive equations shown in the Appendix, the EVP model was enhanced to account for the nonlinear creep behavior.

According to Eq. (6), the enhanced model has one additional parameter m compared with the previous version of Yin et al. (2011b). It is worth pointing out that the parameter m can be determined in a straightforward way based on the conventional oedometer test. Thus, no additional experimental cost is required.

Model Verifications

To evaluate the model's predictive ability, both a laboratory test and an in situ test were simulated by the enhanced model considering the nonlinear creep.

One-Dimensional Creep Test

A conventional oedometer test on a reconstituted sample of Haarajoki clay by Stapelfeldt et al. (2008) was simulated. For reconstituted clays, the destructuration parameters are not needed ($\chi_0 = \xi = \xi_d = 0$). Values of other parameters were determined from conventional oedometer tests (Table 1) and triaxial tests (see Stapelfeldt et al. 2008), as summarized in Table 2. To highlight the improvement by the nonlinear creep formulation, two additional simulations with linear creep ($m = 0$) were carried out using creep coefficient $C_{\alpha ei0} = 0.024$ (initial value corresponding to e_0 of the selected test) and 0.0047 (value corresponding to $\sigma'_v = 640$ kPa), respectively. All simulated results were compared with experimental data in terms of the void ratio-time curves for a 1-day conventional oedometer test, shown in Fig. 7. Note that the same estimated void ratio by models with linear or nonlinear creep consideration at the end of each load with a duration of 1 day is assured by the principle of the model for the case of conventional oedometer test. Thus, the creep rate by different models can be clearly compared with one another.

It is reasonable that the simulated results of linear creep 1 with $C_{\alpha ei0} = 0.024$ and $m = 0$ keep the high creep rate throughout the test, and that the simulated results of linear creep 2 with $C_{\alpha ei0} = 0.0047$ and $m = 0$ keep the low creep rate throughout the test. Only the simulation of nonlinear creep with $C_{\alpha ei0} = 0.024$ and $m = 2.12$ can predict both the decreasing $C_{\alpha e}$ during creep and the consecutively decreasing $C_{\alpha e}$ with applied stresses and soil density. All comparisons show that the consideration of nonlinear creep has well improved the predictive ability of the EVP model.

Table 2. Values of Parameters of Consolidation Model for Selected Test on Haarajoki Clay

M_c	ν'	e_0	κ	λ	$C_{\alpha ei0}$	m	σ'^r_{p0}	τ (h)	k_v (m/h)	c_k
1.23	0.3	2.46	0.046	0.369	0.024	2.12	15	24	3.2×10^{-6}	0.96

Murro Test Embankment

Finite-Element Model

Murro test embankment is an instrumented test embankment on a soft clay deposit, which has been subjected to previous studies (Karstunen et al. 2005; Karstunen and Yin 2010; Yin et al. 2011c). The groundwater table is located at the depth of 0.8 m. The domain to be analyzed (under plane strain conditions) has an extent of 36 m in the horizontal direction from the symmetry axis and 23 m in the vertical direction. The lateral boundaries are restrained horizontally, and the bottom boundary is restrained in both directions (Fig. 8). The finite-element mesh is constituted of 1,456 six-noded triangular elements resulting in 3,019 nodes. A simple linear elastic–perfectly plastic Mohr-Coulomb model was adopted to model the stress-strain behavior of the embankment fill. The typical values of model parameters by Karstunen et al. (2005) are summarized as follows: Young's modulus $E = 40{,}000\,\text{kN/m}^2$, Poisson's ratio $\nu' = 0.35$, critical-state friction angle $\phi'_c = 40°$, dilation angle $\psi = 0°$, and unit weight $\gamma = 19.6\,\text{kN/m}^3$. The embankment loading was reproduced by increasing the unit weight of the elements of the embankment fill (height of 2 m) within 2 days.

Parameters of Foundation Clays

For convenience, in this paper the pre-overburden pressure (POP) defined by POP $= \sigma'^r_{p0} - \sigma'_{v0}$ is used as input instead of σ'^r_{p0} or p^r_{m0}. The initial size p^r_{m0} was computed in the code by the following equation [derived from Eq. (10)]:

$$p^r_{m0} = \left\{ \frac{\left[3 - 3K_0^{nc} - \alpha_{K_0}\left(1 + 2K_0^{nc}\right)\right]^2}{3\left(M_c^2 - \alpha_{K_0}^2\right)\left(1 + 2K_0^{nc}\right)} + \frac{\left(1 + 2K_0^{nc}\right)}{3} \right\} \times \left(\sigma'_{v0} + \text{POP}\right) \tag{7}$$

where $K_0^{nc} = 1 - \sin\phi_c$ with $M_c = 6\sin\phi_c/(3 - \sin\phi_c)$ was assumed (Karstunen and Yin 2010; Yin et al. 2010, 2011b).

Oedometer tests on high-quality intact samples (Karstunen and Yin 2010; Yin et al. 2011c) were selected to determine the

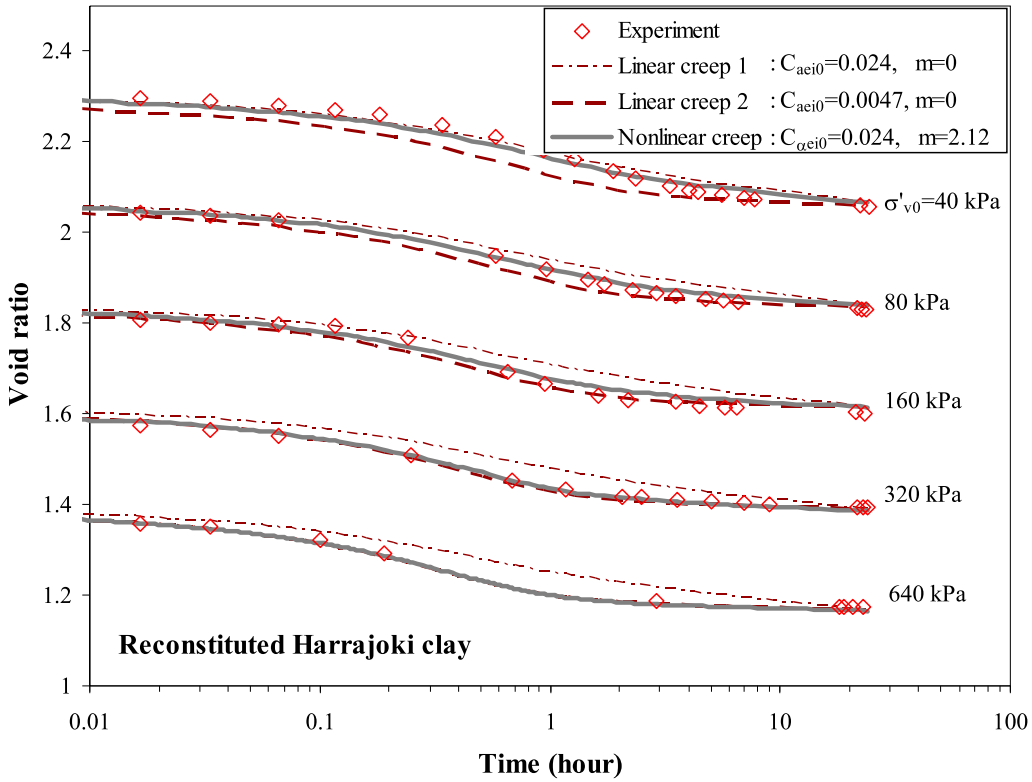

Fig. 7. Test simulations for conventional oedometer test on reconstituted Haarajoki clay

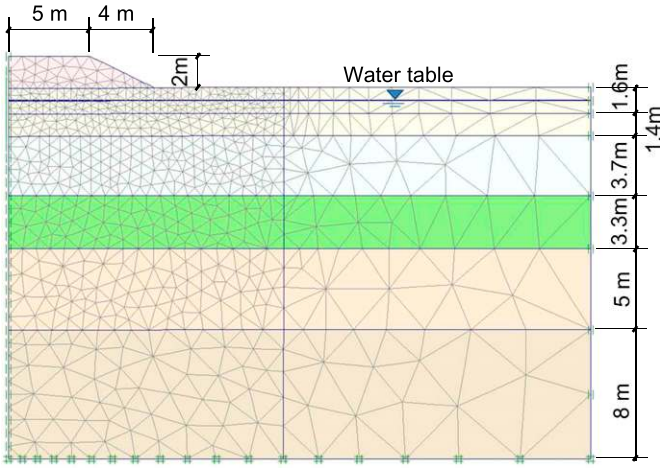

Fig. 8. Finite-element model for Murro test embankment

POP and ξ with assuming $\xi_d = 0.2$, a typical value for Finnish clays proposed by Karstunen et al. (2005) [Fig. 9(a)]. The nonlinear creep parameters $C_{\alpha ei0} = 0.0147$ and $m = 0.73$ corresponding to $e_0 = 2.02$ measured from Murro clay from a depth of 7 m (Table 1) were adopted for all soil layers. Thus, values of $C_{\alpha ei0}$ were obtained by Eq. (5) for all soil layers based on their initial void ratios [Fig. 9(b)]. Values of other parameters determined from various conventional triaxial and oedometer tests for each soil layer by Karstunen and Yin (2010) and Yin et al. (2011c) are adopted and summarized in Tables 3 and 4. The details for the determination of parameters are not repeated in this paper. To investigate the effect of nonlinear creep, two additional predictions were made with different values of m: $m = 0$ and $m = 2.2$. All results were compared with one another.

Settlements

Figs. 10(a and b) show the predicted and measured surface settlements under the centerline of the embankment and 5 m from the centerline of the embankment, respectively. The overpredicted settlements may be attributable to the overestimation of $C_{\alpha ei0}$ for different soil layers, which was not fully investigated experimentally. However, it does not affect the estimation of the influence of nonlinear creep. The major difference was found between the predictions by different considerations of creep behavior after 2,000 days of construction. The difference became more and more significant with time. In general, the prediction considering nonlinear creep with higher value of m results in a smaller settlement because the creep rate reduces more rapidly with the decreasing void ratio. All comparisons show that the consideration of nonlinear creep does not influence the short-term settlement behavior, but influences significantly the long-term settlement behavior.

Horizontal Displacements

Fig. 11 presents the predicted horizontal displacements corresponding to inclinometer I2 by the enhanced model with different considerations of nonlinear creep. At 207 days after the construction, the predicted displacements by all models are almost the same. At 3,201 days after the construction, the model with higher value of m predicted slightly smaller displacements. At 100 years after the construction, the same trend of predicted displacements with m is kept, with the difference becoming more significant. All comparisons show that the influence of consideration of nonlinear creep on the horizontal displacements is less significant than that on settlements. Note that there are differences between measurements and simulations for the horizontal displacements below the depth of

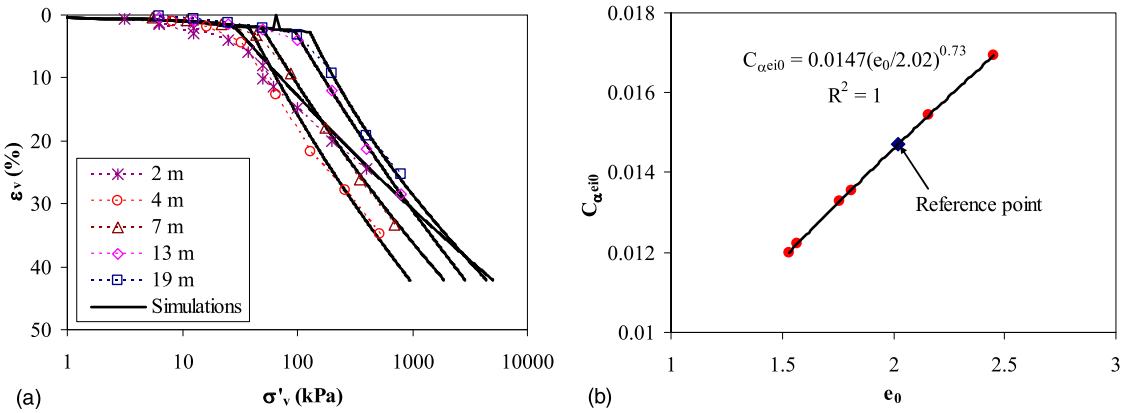

Fig. 9. Determination of parameters: (a) preconsolidation pressure and destructuration parameters from simulating conventional oedometer tests on intact Murro clays of different depths; (b) initial values of creep coefficient for different soil layers with different initial void ratio

Table 3. Values of Parameters of Enhanced EVP Model for Murro Foundation Clays

Depth (m)	γ (kN/m^3)	e_0	M_c	K_0	κ	λ_i	$C_{\alpha ei0}$	m
0.0–1.6	16.1	1.57	1.7	1.25	0.01	0.18	0.0122	0.73
1.6–3.0	15.7	1.81	1.7	0.34	0.024	0.18	0.0136	0.73
3.0–6.7	14.4	2.45	1.65	0.35	0.041	0.25	0.0169	0.73
6.7–10.0	15.2	2.16	1.5	0.40	0.024	0.21	0.0154	0.73
10.0–15.0	15.7	1.76	1.45	0.42	0.024	0.21	0.0133	0.73
15.0–23.0	16.2	1.53	1.4	0.43	0.02	0.15	0.012	0.73

Table 4. Additional Values of Parameters of Enhanced EVP Model for Murro Foundation Clays

Depth (m)	υ'	POP (kPa)	χ_0	ξ	ξ_d	k_v (m/h)	k_h (m/h)	c_k
0.0–1.6	0.3	100	2.5	5	0.2	6.5×10^{-4}	8.3×10^{-4}	0.43
1.6–3.0	0.3	22	6	12	0.2	2.0×10^{-5}	2.6×10^{-5}	0.65
3.0–6.7	0.3	22	6	9	0.2	1.6×10^{-5}	2.2×10^{-5}	0.69
6.7–10.0	0.3	22	6	10	0.2	1.0×10^{-5}	1.4×10^{-5}	0.49
10.0–15.0	0.3	35	4	5	0.2	5.4×10^{-6}	7.2×10^{-6}	0.44
15.0–23.0	0.3	40	6	8	0.2	2.2×10^{-6}	2.9×10^{-6}	0.45

13 m, which may be attributable to the real value of Poisson's ratio of soils less than the assumed value of 0.3 and/or the high stiffness at small strain, and need further investigations.

Excess Pore Pressure

Fig. 12 shows the model predictions with different considerations of nonlinear creep for excess pore pressure in the foundation soil under the centerline at a depth of 9 m. All model predictions are rather similar during the construction and the subsequent consolidation. As expected, all numerical simulations show excess pore pressures gradually dissipating with time. All comparisons show that the influence of consideration of nonlinear creep on the evolution of excess pore pressure is negligible, which is reasonable because the dissipation of excess pore pressure mainly depends on the permeability of foundation soils.

Discussion

Although the predicted settlements and displacements by using all parameters determined from laboratory tests are generally a little bigger than measurements, this does not influence the emphasis of the paper on comparing the linear and nonlinear creep. In fact, for soft sensitive clay, the values of parameters are difficult to estimate accurately owing to the sample disturbance. If the influence of the sample disturbance is accounted for when determining parameters, the prediction will be improved, which needs to be further investigated.

Furthermore, as shown in Fig. 10 combined with Fig. 12, the nonlinear creep influences not only the secondary consolidation stage, but also the primary and the transient stages. For the selected embankment case with available data up to 8 years, the influence of nonlinear creep does not seem significant. However, the influence becomes more and more significant in the long term based on predictions using determined parameters. Although there are no data available with which to compare for long-term settlements, this does not mean that the consideration of nonlinear creep is not needed.

Conclusions

The evolution of creep coefficient has been investigated through conventional oedometer testing on several natural soft clays. All selected clay samples are reconstituted to eliminate the influence of soil structure on the evolution of $C_{\alpha e}$ with applied stress. The nonlinear creep behavior with a consecutively decreasing $C_{\alpha e}$ fully related to the soil density has been clarified. On this basis, a simple nonlinear creep formulation has been proposed.

The proposed nonlinear creep formulation was incorporated into a newly developed EVP model to take into account the nonlinear creep of natural soft clays. The enhanced model has one additional parameter that can be determined from a conventional oedometer test in a straightforward way. No additional experimental cost is required.

The enhanced nonlinear creep model was examined by simulating a conventional oedometer test on reconstituted Haarajoki clay. Simulations with and without consideration of nonlinear creep were compared with experimental results, demonstrating the enhanced model considering nonlinear creep can adequately describe the consecutively decreasing creep coefficient throughout testing. The improvement of predictions by the nonlinear creep formulation was highlighted by comparing predictions with constant $C_{\alpha e}$.

The enhanced model was further applied to an in situ test: Murro test embankment. Model predictions with different values of m ($m = 0, 0.73$, and 2.2) were made to compare with one another. All

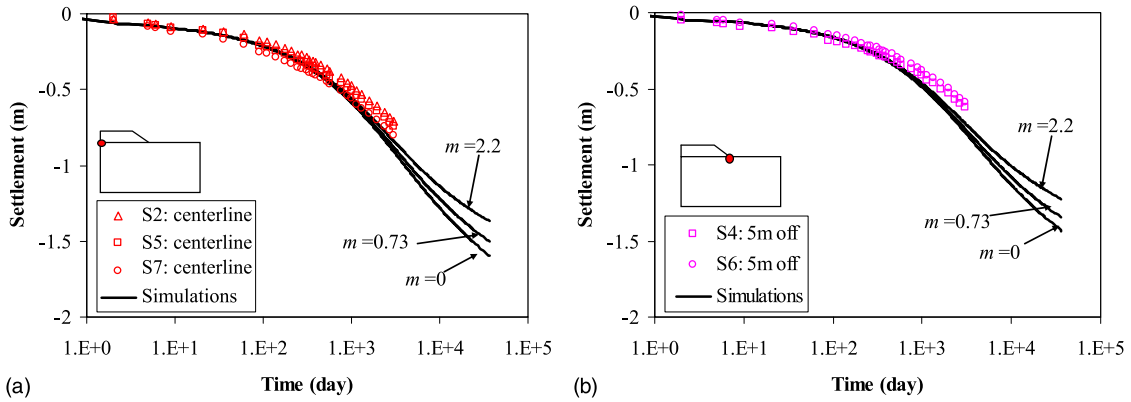

Fig. 10. Settlements: (a) underneath embankment at centerline; (b) underneath embankment 5 m from centerline

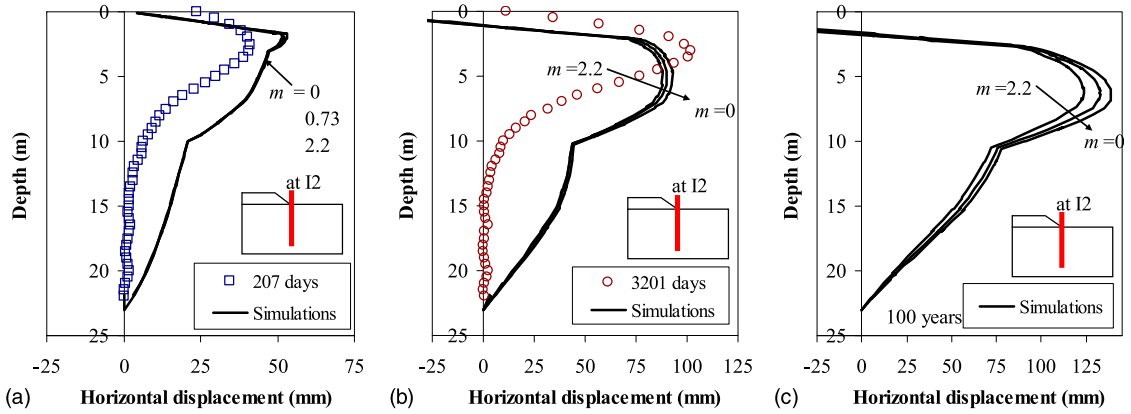

Fig. 11. Horizontal displacements at I2: (a) 207 days after construction; (b) 3,201 days after construction; (c) 100 years after construction

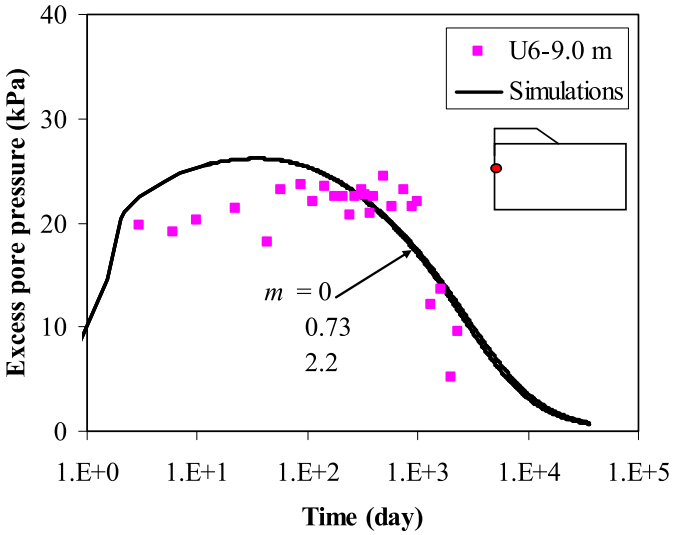

Fig. 12. Excess pore pressures at position U6 (9-m depth under centerline)

comparisons show that (1) for settlements, the consideration of nonlinear creep does not influence the short-term settlement but influences significantly the long-term settlement; (2) the influence of consideration of nonlinear creep on the horizontal displacements is less significant than that on settlements; and (3) the influence of consideration of nonlinear creep on the evolution of excess pore pressure is negligible.

Appendix. Equations and Parameters of EVP Model by Yin et al. (2010, 2011b)

According to Yin et al. (2010, 2011b), the main constitutive equations are listed as follows:

$$\dot{\varepsilon}_{ij} = \dot{\varepsilon}^{e}_{ij} + \dot{\varepsilon}^{vp}_{ij} \tag{8}$$

$$\dot{\varepsilon}^{vp}_{ij} = \mu \left(\frac{p^{d}_{m}}{p^{r}_{m}}\right)^{\beta} \frac{\partial f_d}{\partial \sigma'_{ij}} \tag{9}$$

$$f_r = \frac{(3/2)(\sigma'^{r}_{d} - p'^{r}\alpha_d) : (\sigma'^{r}_{d} - p'^{r}\alpha_d)}{[M^2 - (3/2)\alpha_d : \alpha_d]p'^{r}} + p'^{r} - p^{r}_{m} = 0 \tag{10}$$

$$d\alpha_d = \omega \left[\left(\frac{3\sigma_d}{4p'} - \alpha_d\right) \langle d\varepsilon^{vp}_{v} \rangle + \omega_d \left(\frac{\sigma_d}{3p'} - \alpha_d\right) d\varepsilon^{vp}_{d} \right] \tag{11}$$

$$p^{r}_{m} = (1 + \chi) p_{mi} \tag{12}$$

$$dp_{mi} = p_{mi} \left(\frac{1 + e_0}{\lambda_i - \kappa}\right) d\varepsilon^{vp}_{v} \tag{13}$$

Table 5. State Parameters and Soil Constants of EVP Model

Group	Parameter	Definition	Determination
Modified Cam-clay parameters	σ'^{r}_{p0}	Initial reference preconsolidation pressure (state parameter)	From selected oedometer test corresponding to given reference time (stepwise loading)
	e_0	Initial void ratio (state parameter)	From oedometer test
	υ'	Poisson's ratio	From initial stress-strain curve (typically 0.15–0.35)
	κ	Slope of swelling line	From consolidation test
	λ_i	Intrinsic slope of compression line	From consolidation test on reconstituted samples
	M_c	Slope of critical state line (CSL) in triaxial compression	From triaxial shear test (drained or undrained)
Destructuration parameters	χ_0	Initial amount of bonding (state parameter)	From oedometer test by $\chi_0 = (\sigma'_{p0}/\sigma'_{pi0}) - 1$
	ξ	Absolute rate of bond degradation	From one oedometer test and one isotropic consolidation test
	ξ_d	Relative rate of bond degradation	
Viscosity parameters	$C_{\alpha ei}$	Intrinsic secondary compression coefficient	From conventional oedometer test on reconstituted samples
Hydraulic parameters	k_{v0}, k_{h0}	Initial vertical and horizontal permeability	From oedometer tests
	c_k	Permeability coefficient	From oedometer tests

$$d\chi = -\chi\xi\left(|\, d\varepsilon_v^{vp}\,| + \xi_d d\varepsilon_d^{vp}\right) \tag{14}$$

where $\dot{\varepsilon}_{ij} = (i,j)$ component of the total strain rate tensor; and superscripts e and vp = elastic and viscoplastic components, respectively. The elastic behavior in the proposed model is assumed to be isotropic, similar to the modified Cam-clay model. The p_m^d is the size of the dynamic loading surface. The p_m^r and p_{mi} are the sizes of reference and intrinsic yield surfaces, respectively. The initial reference preconsolidation pressure σ'^{r}_{p0} obtained from the oedometer test can be used as an input to calculate the initial size p_{m0} by following Eq. (10).

Based on the conventional oedometer test for convenience in this paper, the fluidity μ and the strain-rate coefficient β in Eq. (9) are expressed as follows:

$$\mu = \frac{C_{\alpha ei}}{(1+e_0)\tau}\frac{\left(M_c^2 - \alpha_{K_0}^2\right)}{\left(M_c^2 - \eta_{K_0}^2\right)} \quad \text{and} \quad \beta = \frac{\lambda_i - \kappa}{C_{\alpha ei}} \tag{15}$$

The initial value of surface inclination α_0 and values of anisotropy parameters are obtained by

$$\alpha_0 = \alpha_{K_0} = \eta_{K_0} - \frac{M_c^2 - \eta_{K_0}^2}{3} \quad \text{with} \quad \eta_{K_0} = \frac{3M_c}{6 - M_c} \tag{16}$$

$$\omega = \frac{1+e_0}{(\lambda_i - \kappa)}\ln\frac{10M_c^2 - 2\alpha_{K_0}\omega_d}{M_c^2 - 2\alpha_{K_0}\omega_d}$$
$$\text{with} \quad \omega_d = \frac{3\left(4M_c^2 - 4\eta_{K_0}^2 - 3\eta_{K_0}\right)}{8\left(\eta_{K_0}^2 + 2\eta_{K_0} - M_c^2\right)} \tag{17}$$

The slope of critical-state line M is expressed as follows:

$$M = M_c\left[\frac{2c^4}{1 + c^4 + (1 - c^4)\sin 3\theta}\right]^{1/4} \tag{18}$$

where $c = (3 - \sin\phi_c)/(3 + \sin\phi_c)$ according to Mohr-Coulomb yield criterion (ϕ_c = friction angle); and $(-\pi/6) \le \theta = (1/3)\sin^{-1}[(-3\sqrt{3}\bar{J}_3)/(2\bar{J}_2^{3/2})] \le (\pi/6)$ using $\bar{J}_2 = (1/2)\bar{s}_{ij}{:}\bar{s}_{ij}$ and $\bar{J}_3 = (1/3)\bar{s}_{ij}\bar{s}_{jk}\bar{s}_{ki}$ with $\bar{s}_{ij} = \sigma_d - p'\alpha_d$. The model was implemented as a user-defined model in *PLAXIS 2D 9* for a coupled consolidation analysis based on Biot's theory (see details in Yin et al. 2010, 2011a).

During coupled consolidation analyses, the permeability k varies with void ratio e

$$k = k_0 10^{(e-e_0)/c_k} \tag{19}$$

Soil constants and state variables needed as input are summarized in Table 5 with their determination.

Acknowledgments

This research was financially supported by the National Natural Science Foundation of China (Grant No. 41240024, 41372285), the opening project of the State Key Laboratory of Geohazard Prevention and Geoenvironment Protection (Grant No. SKLGP2011K013), Shanghai Pujiang Talent Plan (Grant No. 11PJ1405700), Research Fund for the Doctoral Program of Higher Education of China (Grant No. 20110073120012), and the European project CREEP (PIAPP-GA-2011-286397). This support is greatly appreciated. In addition, the authors thank Professor Minna Karstunen at University of Straithclyde, and Mr. Timo Stapelfeldt and Mr. Matti Lojander at Helsinki University of Technology, for their support.

References

Adachi, T., and Oka, F. (1982). "Constitutive equations for normally consolidated clay based on elasto-viscoplasticity." *Soils Found.*, 22(4), 57–70.

Augustesen, A., Liingaard, M., and Lade, P. V. (2004). "Evaluation of time-dependent behavior of soils." *Int. J. Geomech.*, 10.1061/(ASCE) 1532-3641(2004)4:3(137), 137–156.

Bjerrum, L. (1967). "Engineering geology of Norwegian normally-consolidated marine clays as related to settlements of building." *Geotechnique*, 17(2), 83–118.

Desai, C. S., Sane, S., and Jenson, J. (2011). "Constitutive modeling including creep- and rate-dependent behavior and testing of glacial tills for prediction of motion of glaciers." *Int. J. Geomech.*, 10.1061/(ASCE) GM.1943-5622.0000091, 465–476.

Graham, J., Crooks, J. H. A., and Bell, A. L. (1983). "Time effects on the stress-strain behaviour of natural soft clays." *Geotechnique*, 33(3), 327–340.

Karstunen, M., and Koskinen, M. (2008). "Plastic anisotropy of soft reconstituted clays." *Can. Geotech. J.*, 45(3), 314–328.

Karstunen, M., Krenn, H., Wheeler, S. J., Koskinen, M., and Zentar, R. (2005). "Effect of anisotropy and destructuration on the behavior of Murro test embankment." *Int. J. Geomech.*, 10.1061/(ASCE)1532-3641 (2005)5:2(87), 87–97.

Karstunen, M., and Yin, Z.-Y. (2010). "Modelling time-dependent behaviour of Murro test embankment." *Geotechnique*, 60(10), 735–749.

Kelln, C., Sharma, J. S., Hughes, D., and Graham, J. (2008). "An improved elastic-viscoplastic soil model." *Can. Geotech. J.*, 45(10), 1356–1376.

Kutter, B. L., and Sathialingam, N. (1992). "Elastic-viscoplastic modelling of the rate-dependent behaviour of clays." *Geotechnique*, 42(3), 427–441.

Leoni, M., Karstunen, M., and Vermeer, P. A. (2008). "Anisotropic creep model for soft soils." *Geotechnique*, 58(3), 215–226.

Leroueil, S., Kabbaj, M., Tavenas, F., and Bouchard, R. (1985). "Stress-strain-strain-rate relation for the compressibility of sensitive natural clays." *Geotechnique*, 35(2), 159–180.

Li, J.-Z., Peng, F.-L., and Xu, L. (2009). "One-dimensional viscous behavior of clay and its constitutive modeling." *Int. J. Geomech.*, 10.1061/(ASCE) 1532-3641(2009)9:2(43), 43–51.

Mesri, G., and Godlewski, P. M. (1977). "Time and stress-compressibility interrelationship." *J. Geotech. Engrg. Div.*, 103(5), 417–430.

PLAXIS 2D 9 [Computer software]. Delft, Netherlands, Plaxis.

Roscoe, K. H., and Burland, J. B. (1968). "On the generalized stress–strain behaviour of 'wet' clay." *Engineering plasticity*, J. Heyman and F. A. Leckie, eds., Cambridge University Press, Cambridge, U.K., 553–609.

Stapelfeldt, T., Lojander, M., and Vepsäläinen, P. (2007). "Determination of horizontal permeability of soft clay." *Proc., 17th Int. Conf. on Soil Mechanics and Foundation Engineering*, IOS Press, Amsterdam, Netherlands, 1385–1389.

Stapelfeldt, T., Vepsalainen, P., and Yin, Z.-Y. (2008). "Numerical modelling of a test embankment on soft clay improved with vertical drains." *Proc., 2nd Int. Workshop on Geotechnics of Soft Soils: Focus on Ground Improvement*, M. Karstunen and M. Leoni, eds., Taylor & Francis, London, 173–179.

Vermeer, P. A., and Neher, H. P. (1999). "A soft soil model that accounts for creep." *Proc., Beyond 2000 in Computational Geotechnics—10 Years of Plaxis International*, Balkema, Rotterdam, Netherlands, 249–262.

Yin, J.-H. (1999). "Non-linear creep of soils in oedometer tests." *Geotechnique*, 49(5), 699–707.

Yin, J.-H., and Graham, J. (1989). "Viscous elastic plastic modelling of one-dimensional time dependent behaviour of clays." *Can. Geotech. J.*, 26(2), 199–209.

Yin, J.-H., Zhu, J.-G., and Graham, J. (2002). "A new elastic visco-plastic model for time-dependent behaviour of normally and overconsolidated clays: theory and verification." *Can. Geotech. J.*, 39(1), 157–173.

Yin, Z.-Y., and Chang, C. S. (2009). "Microstructural modelling of stress-dependent behaviour of clay." *Int. J. Solids Struct.*, 46(6), 1373–1388.

Yin, Z.-Y., Chang, C. S., Hicher, P. Y., and Karstunen, M. (2009). "Micromechanical analysis of kinematic hardening in natural clay." *Int. J. Plast.*, 25(8), 1413–1435.

Yin, Z.-Y., Chang, C. S., Karstunen, M., and Hicher, P. Y. (2010). "An anisotropic elastic viscoplastic model for soft soils." *Int. J. Solids Struct.*, 47(5), 665–677.

Yin, Z.-Y., Hattab, M., and Hicher, P. Y. (2011a). "Multiscale modeling of a sensitive marine clay." *Int. J. Numer. Anal. Methods Geomech.*, 35(15), 1682–1702.

Yin, Z.-Y., and Hicher, P. Y. (2008). "Identifying parameters controlling soil delayed behaviour from laboratory and in situ pressuremeter testing." *Int. J. Numer. Anal. Methods Geomech.*, 32(12), 1515–1535.

Yin, Z.-Y., Karstunen, M., Chang, C. S., Koskinen, M., and Lojander, M. (2011b). "Modeling time-dependent behavior of soft sensitive clay." *J. Geotech. Geoenviron. Eng.*, 10.1061/(ASCE)GT.1943-5606.0000527, 1103–1113.

Yin, Z.-Y., Karstunen, M., Wang, J. H., and Yu, C. (2011c). "Influence of features of natural soft clay on the behavior of embankment." *J. Cent. South Univ. Technol.*, 18(5), 1667–1676.